

Spectroscopic Properties of B and B_s meson using Screened Potential

Vikas Patel^{a,b}, Raghav Chaturvedi^c, A. K. Rai^a

^aDepartment of Applied Physics, Sardar Vallabhbhai National Institute of Technology, Surat-395007, Gujarat, INDIA

^bDepartment of Physics, Uka Tarsadia University, Bardoli 394250, Gujarat, INDIA

^c Ministry of Education, Dubai, U.A.E

Received: date / Revised version: date

Abstract. Inspired by the recent observations of B and B_s meson states at LHCb[1] we calculate the masses of ground, orbitally and radially excited states. Also, we estimate the mixing parameters, decay constant, leptonic decay width, and corresponding branching ratios, as well as electromagnetic transition widths. $\mathcal{O}(\frac{1}{m})$ and $\mathcal{O}(p^{10})$ relativistic corrections to potential and kinetic energy terms have been added to the Hamiltonian. The screening potential employed is solved by applying the gaussian wave function. The estimated masses are used to constructed the Regge trajectories, which help us in association of some newly observed states to B and B_s meson family. Overall, the results from present study are in fair agreement with available experimental and theoretical studies.

PACS. PACS-key describing text of that key – PACS-key describing text of that key

1 Introduction

Properties of first two observed states of B-meson, B^0 and B^\pm are well established since their discovery in 1983 at CLEO[2]. After two years lowest-lying vector B-meson (B^*) of $J^P = 1^-$ was observed[3]. The mass difference between ($m_{B^*} - m_B$) is the best measured quantity and its value is 45.18 ± 0.23 . $B_J^*(5732)$ is the first orbitally excited B-meson was observed at OPAL detector at LEP [4]. Later in year 2000 it was studied again at OPAL detector in the $B^* \pi$ invariant mass distribution and the mass was determined to be 5738 ± 7 Mev[5]. In the year 2007, two orbitally excited (L=1) narrow B-mesons were observed at $D\Phi$ in $B^* + \pi^-$ invariant mass distribution[6]. They are $B_1(5721)^0$ with $J^P = 1^+$ and $B_2^*(5747)^0$ with $J^P = 2^+$. In 2013 $B(5970)$ resonance with masses $5978 \pm 5 \pm 12$ Mev for neutral state and $5961 \pm 5 \pm 12$ Mev for the charged state was observed at CDF collaboration in $B^+ \pi^-$ and $B^0 \pi^+$ mass distribution[7]. In the year 2015 LHCb collaboration[8] discovered another excited B-meson $B_J(5960)$. But studies at CDF[7] suggested that $B_J(5960)$ resonances are the same resonant states of $B(5960)$. In addition to $B_J(5970)$ in 2015, the LHCb collaboration[8] also observed another resonant state $B_J(5840)$ with masses $5869 \pm 5 \pm 6.7 \pm 0.2$ Mev for neutral state $B_J(5840)^0$ and $5850.3 \pm 12.7 \pm 13.7 \pm 0.2$ Mev for charged state $B_J(5840)^+$.

In the B_s -meson family the B_s and B_s^* were observed in year 1990 at CUSB-II[9], with masses 5366.82 ± 0.22 Mev and $5415.4^{+1.8}_{-1.5}$ Mev respectively. The first excited B_s -meson was observed in year 1994 as $B_{sJ}^*(5850)$ at LEP in $B^{(*)+} K^-$ invariant mass distribution[4] with mass 5853 ± 15 Mev. Later, at LHCb the first orbitally excited B_s -meson states, $B_{s1}(5830)$ and $B_{s1}(5840)$ with masses 5828.63 ± 0.27 Mev and 5839.85 ± 0.19 Mev were observed at CDF collaboration in 2007[10]. Later, these two states were confirmed by $D\Phi$ and LHCb[11, 12]. Recently, LHCb collaboration [1] observed two new B_s meson states $B_{sJ}(6064)$ and $B_{sJ}(6114)$. In future at LHCb more and more excited B and B_s meson states are expected to be observed due to its vast production cross-section of beauty, together with a good reconstruction efficiency, versatile trigger scheme and an excellent momentum and mass resolution[13]. Listed in Table[1] are the various B and B_s mesons with experimental states, masses and experimental facilities where they were first observed. With increased number of observed new experimental states many theoretical studies have attempted to study B and B_s mesons. The mass spectroscopy has been calculated by various models like relativistic or non-relativistic quark

Send offprint requests to: patelvikas2710@gmail.com

raghavr.chaturvedi@gmail.com

raiajayk@gmail.com

Table 1. B and B_s mesons with experimental states, masses and experimental facilities where they were first observed.

State	J^P	Mass (MeV)	Observed Mode	Experiments
B^\pm	0^-	5279.31 ± 0.15	$D\pi & D^*\pi\pi$	CLEO[36]
B_s^0	0^-	5366.82 ± 0.22		CUSB-II[37]
B^0	0^-	$5279.58 \pm 0.15 \pm 0.28$	$D\pi\pi & D^*\pi$	CLEO[36]
B^*	1^-	5324.65 ± 0.25	$B\gamma$	CUSB[38]
B_s^*	1^-	$5415.4^{+1.8}_{-1.5}$	$B_s\gamma$	CUSB-II[37]
$B_1(5721)^{*\pm}$	1^+	$5725^{+2.5}_{-2.7}$	$B^{*0}\Pi^-$	LHCb[39]
$B_1(5721)^0$	1^+	5726 ± 1.3	$B^{*+}\Pi^-$	CDF[40]
$B_{s1}(5830)$	1^+	$5828.40 \pm 0.04 \pm 0.04 \pm 0.41$	B^*K	LHCb[41]
$B_{s2}^*(5840)^0$	1^+	$5839.99 \pm 0.05 \pm 0.11 \pm 0.17$	B^*K	LHCb[41]
$B_J(5732)$	$?^?$	5695^{+17}_{-19}	$B^*\Pi$	ALEPH[42]
$B_2^*(5747)^+$	2^+	$5737.20 \pm 0.72 \pm 0.40 \pm 0.17$	$B^{*0}\Pi^+$	LHCb[39]
$B_{sJ}^*(5850)$	$?$	5853 ± 15		OPAL[43]
$B_2^*(5747)^0$	2^+	$5739.44 \pm 0.37 \pm 0.33 \pm 0.17$	$B^{*+}\Pi^+$	LHCb[39]
$B_J(5840)^+$	$?^?$	$5850.3 \pm 12.7 \pm 13.7 \pm 0.2$	$B\Pi$	LHCb[39]
$B_J(5840)^0$	$?^?$	$5862.9 \pm 5.0 \pm 6.7 \pm 0.2$	$B\Pi$	LHCb[39]
$B_J(5970)^+$	$?^?$	$5961 \pm 5 \pm 12$	$B^0\Pi^+$	CDF[40]
$B_J(5970)^0$	$?^?$	$5978 \pm 5 \pm 12$	$B^+\Pi^-$	CDF[40]
$B_{sJ}(6064)^0$	$?^?$	$6063.5 \pm 1.2 \pm 0.8$	B^+K^-	LHCb[1]
$or B_{sJ}(6109)^0$	$?^?$	$6108.8 \pm 1.1 \pm 0.7$	$B^{*+}K^-$	LHCb[1]
$B_{sJ}(6114)^0$	$?^?$	$6114 \pm 3 \pm 5$	B^+K^-	LHCb[1]
$or B_{sJ}(6158)^0$	$?^?$	$6158.5 \pm 4 \pm 5$	$B^{*+}K^-$	LHCb[1]

models, potential model, Bethe-Salpeter equation as well as constituent quark model[6,14,10,8,13,15,16,17,18,19]. Also, the strong decays, radiative decays, and semileptonic decays have been calculated theoretically[20,21,22,23,24,25,26].

$B_1(5721)$, $B_2^*(5747)$, $B_{S1}(5830)$, $B_{S2}^*(5840)$ are well entrenched states and various quark model studies [26,27,28,20,21,22,23,29,30,31] have tried to prove them as first excitations of B and B_s meson. Since, their discovery at CDF and LHCb, based on their observed masses and decay properties, theoretical studies have associated $B_J(5840)$ as $B(2^1S_0)$ [22,23,32,33], $B(2^3S_1)$ by [34], or $B(1^3D_1)$ by [32]. Whereas, $B_J(5960)^0$ is associated as $B(2^3S_1)$ by [27,20,32], $B(1^3D_3)$ by [22,34], or $B(1^3D_1)$ by [23,35]. Their is only one theoretical study about newly observed B_s meson states, $B_{sJ}(6064)$ and $B_{sJ}(6114)$. Thus, providing us inspiration to study the B and B_s meson spectroscopy. In this article we employ screening potential to study the mass spectroscopy and various decay properties of B and B_s mesons. We expect that for the light quark confining term will play a crucial role along with usual Coulombic term. Also, the screening potential will help to study the effective quenching between the quark and anti-quark. We then solve the potential using the variational approach. We also include $\mathcal{O}(p^{10})$ relativistic correction to kinetic energy and potential energy terms in the Hamiltonian. The Regge trajectories are constructed to help the association of new experimental observed states to the B and B_s meson family. We also estimate the pseudoscalar and vector decay constants as these decay constants are very important for calculating various weak decay properties. The leptonic branching ratio (BR) and electromagnetic (EM) transitions are also calculated in this scheme.

After introduction, Section 2 deals with theoretical framework to calculate the mass spectroscopy. Section 3 contains Regge trajectories. Section 4 accomodates calculations for decay constant. In Section 5 the leptonic branching fractions are computed. Section 6 deals with mixing parameters' calculations. In Section 7, calculation of electromagnetic transition widths are discussed and finally, in Section 8 results, discussion and conclusion are presented.

2 Theoretical framework for Mass Spectroscopy calculation

We use the below mentioned Hamiltonian to calculate the B and B_s meson mass spectrum[44],

$$H = \sqrt{p^2 + m_1^2} + \sqrt{p^2 + m_2^2} + V(\mathbf{r}); \quad (1)$$

m_1 and $m_{\bar{m}_2}$ are the heavy(b, \bar{b}) and light quark($u, \bar{u}, d, \bar{d}, s, \bar{s}$) masses, p is the relative momentum of the quark and anti-quark system, and $V(\mathbf{r})$ is the quark anti-quark interaction potential. To accompany the relativistic effects the kinetic energy term in the Hamiltonian has been expanded to $\mathcal{O}(p^{10})$. In Table 3 we list down the contribution to

the Hamiltonian due to various orders in p ($\mathcal{O}(p)$). Except $\mathcal{O}(p^2)$ the leading terms in $\mathcal{O}(p)$ have shrinking values, but because $\mathcal{O}(p^4)$ and $\mathcal{O}(p^8)$ terms are negative and $\mathcal{O}(p^6)$ and $\mathcal{O}(p^{10})$ terms are positive, they may have cancelling effect on each other, as a consequence we feel the term $\mathcal{O}(p^{10})$ may play a significant role in the mass spectroscopy calculation. The quark anti-quark potential is of the form[45],

$$V(r) = V^{(0)}(r) + \left(\frac{1}{m_1} + \frac{1}{m_{\bar{2}}} \right) V^{(1)}(r) + \mathcal{O}\left(\frac{1}{m^2}\right); \quad (2)$$

Where, $V^{(0)}$ is the spin-independent potential between the quark and anti-quark[46], $V_v(r)$ is Lorentz vector and $V_s(r)$ is Lorentz scalar contribution.

$$V^{(0)}(r) = V_v(r) + V_s(r) + V_0; \quad (3)$$

$$V_v(r) = -\frac{\alpha_c}{r} \quad (4)$$

$$V_s(r) \equiv \begin{cases} Ar & \text{linear} \\ \frac{A}{\mu}(1 - e^{-\mu r}) & \text{screened;} \end{cases} \quad (5)$$

It has been interpreted by theoretical studies[47,48], at distances greater than 1 fm the spontaneous creation of light quark anti-quark pairs inside a meson softens linear confinement potential by screening a colour charge. Hence, we research the effect of screening on linear confinement potential at larger distances in the quark anti-quark interaction. In present article we modify the Cornell potential by incorporating the Screening effect and calculate the ground and excited state masses for B and B_s mesons. At distance $r \ll 1/\mu$, $V_s(r)$ behave like linear potential ($A(r)$) and for $r \gg 1/\mu$, $V_s(r)$ becomes constant. Where, “ μ ” is the screening factor and its value during the mass spectra calculation is taken as 0.04, and V_0 is potential constant. To justify why the value of “ μ ” is taken as 0.04 during the mass spectra calculation for B and B_s meson, masses for various states of have been calculated for different values of “ μ ” and are tabulated in Tables 4 and 5, the calculated masses from the present work matches well with the experimental masses for $\mu = 0.04$. Also, the $\chi^2/d.o.f$ or the goodness of fit values for different “ μ ” values for B and B_s mesons have been calculated. The $\chi^2/d.o.f$ is calculated as per [49], $\chi^2/d.o.f = \sum \frac{(\text{observed} - \text{expected})^2}{\text{expected}}$. Here, observed values are the predicted values for various μ 's and expected values are the experimental masses, Minimum value for $\chi^2/d.o.f$ is obtained for $\mu = 0.04$. Hence, validating the choice of “ μ ” as 0.04. α_c and α_s are effective running and running coupling constants determined through the simplest model with freezing[50,51,52]. α_c and α_s follow the relation $\alpha_c = 4/3\alpha_s$. Λ , the QCD scales taken as 0.413 GeV. n_f is the number of flavors and M is the re-normalisation scale related to the constituent quark masses as $M = 2m_Q m_{\bar{q}} / (m_Q + m_{\bar{q}})$ [52]. A in Eq. 5 represents potential strength.

$$\alpha_s(\mu)^2 = \frac{4\pi}{\left(11 - \frac{2}{3}n_f\right) \ln \frac{M^2 + M_B^2}{\Lambda^2}} \quad (6)$$

$V^{(1)}(r)$ in Eq. 2 is a relativistic correction taken as,

$$V^{(1)}(r) = -C_1 C_2 \alpha_s^2 / 4r^2 \quad (7)$$

$C_1 = 4/3$ and $C_2 = 3$ are the Casimir charges. The values of all the potential parameters used in the present work are listed in Table 2. In the present work Gaussian like wave-function in position and momentum space has been used, see Eqs. 8 & 9. Where, “ u ” and “ L ” are variational parameter and Laguerre polynomial, respectively. Ritz variational scheme has been used. And, the expectation value is obtained as $H\psi = E\psi$.

$$R_{nl}(u, r) = u^{3/2} \left(\frac{2(n-1)!}{\Gamma(n+l+1/2)} \right)^{1/2} (ur)^l \times e^{-u^2 r^2 / 2} L_{n-1}^{l+1/2}(u^2 r^2); \quad (8)$$

$$R_{nl}(u, p) = \frac{(-1)^n}{u^{3/2}} \left(\frac{2(n-1)!}{\Gamma(n+l+1/2)} \right)^{1/2} \left(\frac{p}{u} \right)^l e^{-p^2 / 2u^2} L_{n-1}^{l+1/2} \left(\frac{p^2}{u^2} \right); \quad (9)$$

The values of the variational parameter “ u ” has been found graphically using the virial theorem[53]. The values for “ u ” can be found in Table 6. The Gaussian wave function in the position space is employed to obtain the expectation

value of potential energy. Whereas, the Gaussian wave function in the momentum space is employed to obtain the expectation value of kinetic energy.

$$\langle K.E. \rangle = \frac{1}{2} \left\langle \frac{rdV}{dr} \right\rangle. \quad (10)$$

Equation 11 is employed to determine the spin-average mass for the ground state[54]. The potential constant V_0 in Eq. 3 is fixed to obtain the experimental spin-averaged mass. The expectation value of the Hamiltonian yield spin-average mass. The calculated spin-average masses can be found in Table 6.

$$M_{SA} = M_{PS} + \frac{3}{4}(M_{Vec} - M_{PS}) \quad (11)$$

We compute the spin-average mass from the respective theoretical values as per Eq.13 in Ref.[54] for the comparison for the nJ state,

$$M_{CW,n} = \frac{\Sigma_J(2J+1)M_{nJ}}{\Sigma_J(2J+1)} \quad (12)$$

where, $M_{CW,n}$ and M_{nJ} denotes the spin-averaged mass of the n state, and the mass of the meson in the nJ state, respectively.

$$M_{CW,n} = \frac{\Sigma_J(2J+1)M_{nJ}}{\Sigma_J(2J+1)} \quad (13)$$

We add perturbatively the spin-dependent potential to calculate the hyperfine and spin-orbit splitting which is of the form[55],

$$\begin{aligned} V_{spin}(r) = & \left(\frac{L \cdot S_1}{2m_1^2} + \frac{L \cdot S_2}{2m_2^2} \right) \left(-\frac{dV^{(0)}(r)}{rdr} + \frac{8}{3}\alpha_S \frac{1}{r^3} \right) + \\ & \frac{4}{3}\alpha_S \frac{1}{m_1 m_2} \frac{L \cdot S}{r^3} + \frac{4}{3}\alpha_S \frac{2}{3m_1 m_2} S_1 \cdot S_2 4\pi\delta(r) \\ & + \frac{4}{3}\alpha_S \frac{1}{m_1 m_2} \left\{ 3(S_1 \cdot n)(S_2 \cdot n) - (S_1 \cdot S_2) \right\} \frac{1}{r^3}, \quad n = \frac{r}{r}; \end{aligned} \quad (14)$$

The first term in Eq. 14 is the relativistic correction to the potential $V^{(0)}$, the second term considers the spin-orbit interaction, the third and the fourth terms are for spin-spin and tensor interactions. The heavy-heavy flavored meson states with $J = L$ are mixtures of spin-triplet $|^3L_L\rangle$ and spin-singlet $|^1L_L\rangle$ states: $J = L = 1, 2, 3, \dots$

$$|\psi_J\rangle = |^1L_L\rangle \cos\theta + |^3L_L\rangle \sin\theta \quad (15)$$

$$|\psi'_J\rangle = -|^1L_L\rangle \sin\theta + |^3L_L\rangle \cos\theta \quad (16)$$

where, “ θ ” is the mixing angle and the primed state has the heavier mass. Such mixing occurs due to the nondiagonal spin-orbit and tensor terms in Eq.14. The calculated masses can be found in Tables 7, 8, 9 & 10.

Table 2. Potential Parameters

Meson	α_s	α_c	$m_{u/d}$ (GeV)	m_s (GeV)	m_b (GeV)	nf	Λ	μ	A (GeV ²)	V_0
B	0.732	0.976	0.46		4.53	5	0.413	0.04	0.16	-0.095
B_s	0.668	0.891		0.586	4.53	5	0.413	0.04	0.16	0.004

Table 3. 1S, 2S & 1P spin-average masses of B and B_s mesons considering various orders of $\mathcal{O}(p)$.

state	B -meson				B_s -meson			
	$\mathcal{O}(p^4)$	$\mathcal{O}(p^6)$	$\mathcal{O}(p^8)$	$\mathcal{O}(p^{10})$	$\mathcal{O}(p^4)$	$\mathcal{O}(p^6)$	$\mathcal{O}(p^8)$	$\mathcal{O}(p^{10})$
1S	4667	4808	4523	5314	4800	5949	5667	5401
2S	5448	5626	5326	5959	5567	5741	5475	5990
1P	5455	5571	5385	5779	5596	5701	5550	5838
1D	5794	5922	5729	6104	5923	6033	5886	6139

Table 4. Masses for B meson for various μ from 0.01 till 0.05.

state	0.01	0.02	0.03	0.04	0.05
1^1S_0	5378	5322	5290	5282	5275
1^3S_1	5364	5364	5331	5324	5317
2^1S_0	6163	6069	5981	5951	5923
2^3S_1	6174	6080	5991	5962	5934
3^1S_0	6832	6589	6511	6449	6391
3^3S_1	6837	6593	6516	6453	6396
1^3P_0	5810	5790	5771	5752	5735
1^3P_1	5822	5803	5784	5766	5748
1^1P_1	5837	5818	5800	5783	5766
1^3P_2	5835	5815	5797	5779	5762
2^3P_0	6442	6389	6338	6291	6247
2^3P_1	6449	6396	6346	6299	6255
2^1P_1	6457	6404	6355	6309	6247
2^3P_2	6456	6403	6354	6307	6263
1^3D_1	6210	6176	6143	6112	6083
1^3D_2	6199	6164	6134	6104	6075
1^1D_2	6198	6164	6132	6102	6074
1^3D_3	6195	6163	6132	6102	6073
2^3D_1	6787	6711	6642	6577	6517
2^3D_2	6778	6703	6635	6571	6511
2^1D_2	6778	6703	6634	6570	6510
2^3D_3	6774	6700	6632	6569	6510
1^3F_2	6527	6746	6428	6383	6340
1^3F_3	6515	6765	6418	6374	6332
1^1F_3	6513	6764	6417	6373	6331
1^3F_4	6505	6457	6411	6368	6327

3 Regge Trajectories

Using the calculated masses from the present approach we build up Regge trajectories in $(J \rightarrow M^2)$ and $(n_r \rightarrow M^2)$ planes. To construct the Regge trajectories we use the definitions $J = \alpha M^2 + \alpha_0$ and $n_r \equiv n - 1 = \beta M^2 + \beta_0$. Here, α_0, β_0 are intercepts, and α, β are the slopes. The natural and un-natural parity Regge trajectories in for $(J \rightarrow M^2)$ planes for B and B_s mesons can be found in figures 1, 2, 5, and 6. Whereas, the Regge trajectories in $(n_r \rightarrow M^2)$ planes for B and B_s mesons can be found in figures 3, 4, 7 and 8. The calculated values of slopes and intercepts can be found in Tables 11, 12 and 13.

4 Decay Constant

The decay constants are important parameters for studying the leptonic and non-leptonic decay processes. After incorporating the first order QCD corrections the decay constants for various states have been calculated by using the Van-Royen-Weisskopf formula[58].

$$f_{p/v}^2 = \frac{12 |\psi_{P/V}(0)|^2}{M_{P/V}} \bar{C}^2(\alpha_S), \quad (17)$$

Table 5. Masses for B_s meson for various μ from 0.01 till 0.05.

state	0.01	0.02	0.03	0.04	0.05
1^1S_0	5374	5369	5364	5359	5354
1^3S_1	5329	5424	5420	5415	5410
2^1S_0	6044	6021	6000	5980	5960
2^3S_1	6057	6035	6014	5993	5973
3^1S_0	6580	6530	6483	6438	6397
3^3S_1	6586	6536	6488	6444	6403
1^3P_0	5838	5824	5831	5798	5785
1^3P_1	5858	5844	5811	5818	5806
1^1P_1	5884	5871	5828	5846	5834
1^3P_2	5877	5864	5851	58389	5826
2^3P_0	6399	6361	6326	6292	6260
2^3P_1	6410	6373	6338	6304	6272
2^1P_1	6425	6388	6323	6320	6289
2^3P_2	6422	6350	6349	6316	6284
1^3D_1	6203	6179	6157	6144	6144
1^3D_2	6205	6190	6167	6139	6123
1^1D_2	6214	6182	6160	6135	6119
1^3D_3	6206	6183	6160	6139	6118
2^3D_1	6706	6653	6603	6564	6513
2^3D_2	6718	6661	6611	6560	6520
2^1D_2	6706	6654	6605	6557	6516
2^3D_3	6707	66655	6606	6559	6516
1^3F_2	6496	6460	6425	6392	6361
1^3F_3	6486	6450	6416	6384	6353
1^1F_3	6486	6450	6417	6385	6354
1^3F_4	6479	6445	6412	6381	6351

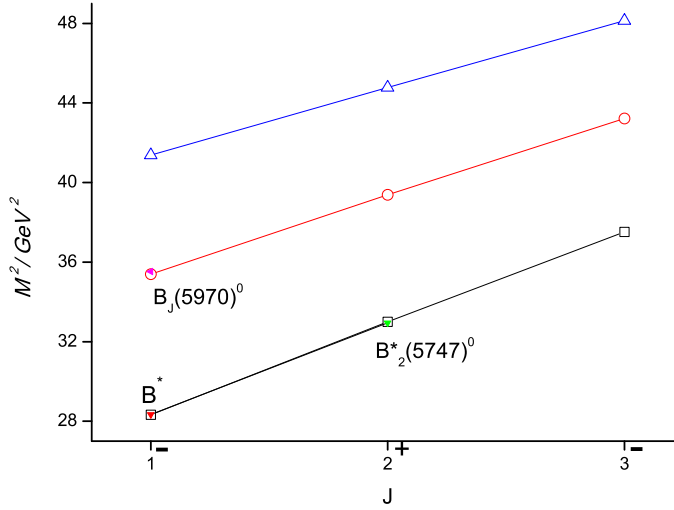


Fig. 1. $J \rightarrow M^2$ Regge trajectory for B -meson, natural parity states, hollow shapes indicates present results and solid shapes indicates experimental results

Table 6. Spin average masses for S, P, D and F states in B and B_s mesons (in MeV).

Meson	State	$\mu(\text{MeV})$	$M_{SA}(\text{MeV})$	[56]	[16]	[57]	[17]	[27]
B	1S	390	5314	5314	5314	5314	5314	5288
	2S	281	5951	5944	5942	5819	5902	5903
	3S	231	6452		6504	6251	6385	
	4S	200	6846		6772		6785	
	5S	179	7165		7546		7132	
	6S	163	7427					
	1P	314	5779	5730	5740	5737	5745	5759
	2P	247	6307		6301	6127	6249	6188
	3P	211	6726		6828	6482	6669	
	4P	187	7068					
	5P	169	7348					
	1D	280	6104		6057	6045	6106	6042
	2D	229	6571		6596	6429	6540	6377
	3D	199	6944		7110	6769		
	4D	178	7249					
5D	162	7500						
B	1F	258	6343					
	2F	215	6798					
	3F	189	7136					
	4F	171	7411					
	5F	157	7642					
B_s	1S	481	5401	5401	5401	5403	5404	5370
	2S	342	5990		6023	5952	5988	5971
	3S	280	6443		6570	6425	6473	
	4S	242	6788		7083	6863	6878	
	5S	219	7117		7575			
	6S	200	7376					
	1P	379	5838	5840	5835	5838	5844	5838
	2P	294	6316		6380	6233	6343	6254
	3P	255	6701		6889	6603	6768	
	4P	227	7023					
	5P	206	7295					
	1D	335	6139		6150	6181	6200	6117
	2D	275	6560		6668	6626	6635	6450
	3D	240	6905		7162	6912		
	4D	216	7358					
5D	198	7444						
B_s	1F	307	6385					
	2F	259	6769					
	3F	229	7085					
	4F	208	7352					
	5F	191	7579					

Table 7. S and P states mass spectrum of B meson (in MeV).

State	J^P	Meson	Present	[56]	[16]	[57]	[17]	[21]	[27]
1^1S_0	0^-	B^0 B^\pm	5282	5279 ± 0.015 5279 ± 0.014	5287	5289	5280	5312	5273
2^1S_0	0^-	$B_J(5840)^0$	5951	5860 ± 0.081	5926	5804	5840	5904	5893
3^1S_0	0^-		6449		6492	6242	6379	6335	
4^1S_0	0^-		6844		7027	6641	6781	6689	
5^1S_0	0^-		7164		7538			6997	
6^1S_0	0^-		7426						
1^3S_1	1^-	B^*	5324	5324 ± 0.25	5323	5325	5326	5371	5331
2^3S_1	1^-	$B_J(5970)^+$ $B_J(5970)^0$	5962	5967 ± 5 5971 ± 5	5947	5834	5906	5933	5932
3^3S_1	1^-		6453		6508	6254	6387	6355	
4^3S_1	1^-		6846		7039	6649	6786	6703	
5^3S_1	1^-		7165		7549			7008	
6^3S_1	1^-		7427						
1^3P_0	0^+		5752	$5732^{+0.005}_{-0.02}$	5730	5697	5749	5756	5740
1^1P_1	1^+	$B_1(5721)^0$	5766	$5725^{+2.5}_{-2.7}$	5733	5723	5723	5777	5815
1^3P_1	1^+		5783	5726 ± 1.3	5752	5738	5774	5784	5731
1^3P_2	2^+	$B_2^*(5747)^+$ $B_2^*(5747)^0$	5779	5737 ± 0.7 5739 ± 0.7	5740	5754	5741	5797	5746
2^3P_0	0^+		6291		6297	6053	6221	6213	6188
2^1P_1	1^+		6299		6295	6106	6209	6197	6168
2^3P_1	1^+		6309		6311	6131	6281	6228	6221
2^3P_2	2^+		6307		6299	6153	6260	6213	6179
3^3P_0	0^+		6715		6826	6375	6629	6576	
3^1P_1	1^+		6721		6829	6453	6650	6557	
3^3P_1	1^+		6727		6837	6486	6685	6585	
3^3P_2	2^+		6726		6826	6518	6678	6570	
4^3P_0	0^+		7059					6890	
4^1P_1	1^+		7063					6872	
4^3P_1	1^+		7068					6897	
4^3P_2	2^+		7068					6883	
5^3P_0	0^+		7341						
5^1P_1	1^+		7344						
5^3P_1	1^+		7348						
5^3P_2	2^+		7348						

Table 8. D and F states mass spectrum of B meson (in MeV).

State	J^P	Meson	Present	[56]	[16]	[57]	[17]	[21]	[27]
1^3D_1	1^-		6112		6016	6104	6119	6110	6135
1^1D_2	2^-		6104		6031	6076	6121	6095	5967
1^3D_2	2^-		6102		6065	6065	6103	6124	6152
1^3D_3	3^-		6102		6085	6041	6091	6106	5976
2^3D_1	1^-		6577		6562	6460	6534	6475	6445
2^1D_2	2^-		6571		6575	6440	6554	6450	6323
2^3D_2	2^-		6570		6602	6429	6528	6486	6456
2^3D_3	3^-		6569		6619	6409	6542	6460	6329
3^3D_1	1^-		6949		7081	6795		6792	
3^1D_2	2^-		6944		7093	6768		6767	
3^3D_2	2^-		6944		7116	6779		6800	
3^3D_3	3^-		6943		7130	6751		6775	
4^3D_1	1^-		7253						
4^1D_2	2^-		7249						
4^3D_2	2^-		7248						
4^3D_3	3^-		7248						
5^3D_1	1^-		7503						
5^1D_2	2^-		7500						
5^3D_2	2^-		7500						
5^3D_3	3^-		7499						
1^3F_2	2^+		6383					6387	
1^1F_3	3^+		6374					6358	
1^3F_3	3^+		6373					6396	
1^3F_4	4^+		6368					6364	
2^3F_2	2^+		6805					6704	
2^1F_3	3^+		6798					6673	
2^3F_3	3^+		6798					6711	
2^3F_4	4^+		6793					6679	
3^3F_2	2^+		7141						
3^1F_3	3^+		7136						
3^3F_3	3^+		7136						
3^3F_4	4^+		7132						
4^3F_2	2^+		7416						
4^1F_3	3^+		7411						
4^3F_3	3^+		7411						
4^3F_4	4^+		7408						
5^3F_2	2^+		7646						
5^1F_3	3^+		7642						

Table 9. S and P states mass spectrum of B_s meson (in MeV).

State	J^P	Meson	Present	[56]	[16]	[57]	[17]	[21]	[27]
1^1S_0	0^-	B_S^0	5359	5366 ± 0.19	5367	5366	5372	5394	5355
2^1S_0	0^-		5980		6003	5939	5976	5984	5962
3^1S_0	0^-		6438		6556	6419	6467	6410	6415
4^1S_0	0^-		6786		7071	6859	6874	6759	
5^1S_0	0^-		7116		7565			7063	
6^1S_0	0^-		7375						
1^3S_1	1^-	B_S^*	5415	$5415_{-1.5}^{+1.8}$	5413	5415	5414	5440	5416
2^3S_1	1^-		5993		6029	5956	5992	6012	5999
3^3S_1	1^-		6444		6575	6427	6475	6429	
4^3S_1	1^-		6789		7087	6864	6879	6773	
5^3S_1	1^-		7118		7579			7076	
6^3S_2	1^-		7376						
1^3P_0	0^+		5798		5812	5799	5833	5831	5782
1^1P_1	1^+	$B_{S1} (5830)^0$	5818	5828 ± 0.27	5828	5819	5865	5857	5833
1^3P_1	1^+	B_{sJ}^*	5846	5850	5842	5854	5831	5861	5843
1^3P_2	2^+	$B_{S2}^* (5840)^0$	5838	5839 ± 0.17	5840	5849	5842	5876	5848
2^3P_0	0^+		6292		6367	6171	6348	6279	6220
2^1P_1	1^+		6304		6375	6197	6345	6279	6250
2^3P_1	1^+		6320		6387	6278	6321	6296	6256
2^3P_2	2^+		6316		6382	6241	6359	6295	6261
3^3P_0	0^+		6684		6879	6510	6731	6639	
3^1P_1	1^+		6693		6885	6663	6761	6635	
3^3P_1	1^+		6704		6895	6543	6768	6650	
3^3P_2	2^+		6701		6890	6622	6780	6648	
4^3P_0	0^+		7009					6950	
4^1P_1	1^+		7016					6946	
4^3P_1	1^+		7025					6959	
4^3P_2	2^+		7023					6956	
5^3P_0	0^+		7283						
5^1P_1	1^+		7289						
5^3P_1	1^+		7297						
5^3P_2	2^+		7295						

where, $\bar{C}^2(\alpha_S)$ is the QCD correction factor given by [59]. The calculated values of the decay constant for B and B_s meson can be found in Table 14.

5 Leptonic, Radiative leptonic and Dileptonic Branching fractions

The leptonic branching fraction is calculated using the formula,

$$BR = \Gamma \times \tau \quad (18)$$

Table 10. D and F states mass spectrum of B_s meson (in MeV).

State	J^P	Meson	Present	[56]	[16]	[57]	[17]	[21]	[27]
1^3D_1	1^-	$B_{sJ}(6064)$	6144		6119	6226	6209	6179	6155
1^1D_2	2^-		6139		6128	6177	6218	6169	6079
1^3D_2	2^-		6135		6157	6209	6189	6196	6172
1^3D_3	3^-		6139		6172	6145	6191	6179	6088
2^3D_1	1^-		6564		6642	6595	6629	6542	6478
2^1D_2	2^-		6560		6650	6554	6651	6526	6422
2^3D_2	2^-		6557		6674	6585	6625	6553	6490
2^3D_3	3^-		6559		6687	6528	6637	6535	6429
3^3D_1	1^-		6909		7139	6942		6855	
3^1D_2	2^-		6905		7147	6907		6841	
3^3D_2	2^-		6904		7167	6936		6864	
3^3D_3	3^-		6905		7178	6885		6849	
4^3D_1	1^-		7361						
4^1D_2	2^-		7358						
4^3D_2	2^-		7456						
4^3D_3	3^-		7358						
5^3D_1	1^-	7447							
5^1D_2	2^-	7444							
5^3D_2	2^-	7443							
5^3D_3	3^-	7444							
1^3F_2	2^+		6392					6454	
1^1F_3	3^+		6384					6425	
1^3F_3	3^+		6385					6462	
1^3F_4	4^+		6381					6432	
2^3F_2	2^+		6775					6768	
2^1F_3	3^+		6769					6742	
2^3F_3	3^+		6769					6775	
2^3F_4	4^+		6765					6748	
3^3F_2	2^+		7090						
3^1F_3	3^+		7085						
3^3F_3	3^+		7085						
3^3F_4	4^+		7082						
4^3F_2	2^+		7357						
4^1F_3	3^+		7352						
4^3F_3	3^+		7352						
4^3F_4	4^+		7350						
5^3F_2	2^+		7582						
5^1F_3	3^+		7579						
5^3F_3	3^+		7579						

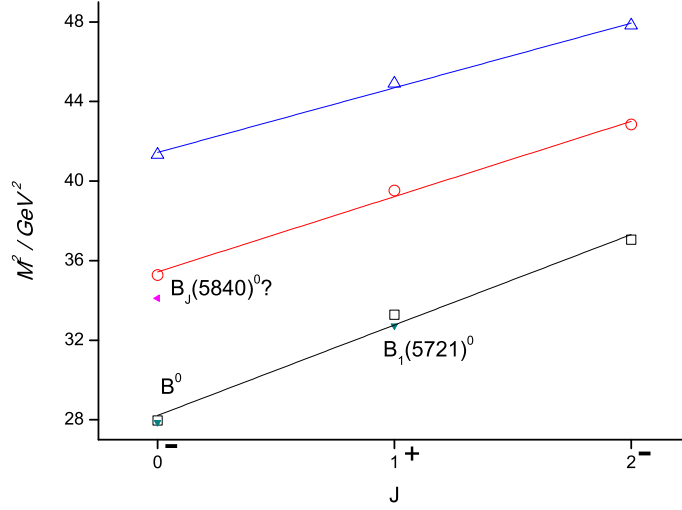


Fig. 2. $J \rightarrow M^2$ Regge trajectory for B -meson, un-natural parity states, hollow shapes indicates present results and solid shapes indicates experimental results

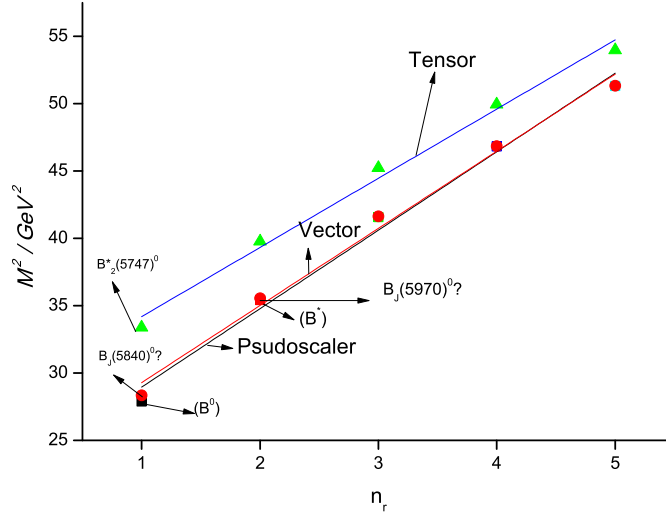


Fig. 3. $n_r \rightarrow M^2$ Regge trajectory for B -meson, pseudoscalar, vector and tensor states

The leptonic decay width(Γ) is given as per[67]. Calculated leptonic branching fraction can be found in Table 15.

$$\Gamma(B^+ \rightarrow l^+ \nu_l) = \frac{G_F^2}{8\pi} f_B^2 |V_{ub}|^2 m_l^2 \times \left(1 - \frac{m_l^2}{M_B^2}\right)^2 M_B \quad (19)$$

The radiative leptonic decay width $B^- \rightarrow \gamma l \bar{\nu}$ ($l = e, \mu$) is calculated as per[68]. The results can be found in Table 16.

$$\Gamma(B^- \rightarrow \gamma l \bar{\nu}) = \frac{\alpha G_F^2 |V_{bu}|^2}{2592\pi^2} f_B^2 m_B^3 [x_u + x_b], \quad (20)$$

where

$$x_u = \left(3 - \frac{m_{B^-}}{m_u}\right)^2, \quad (21)$$

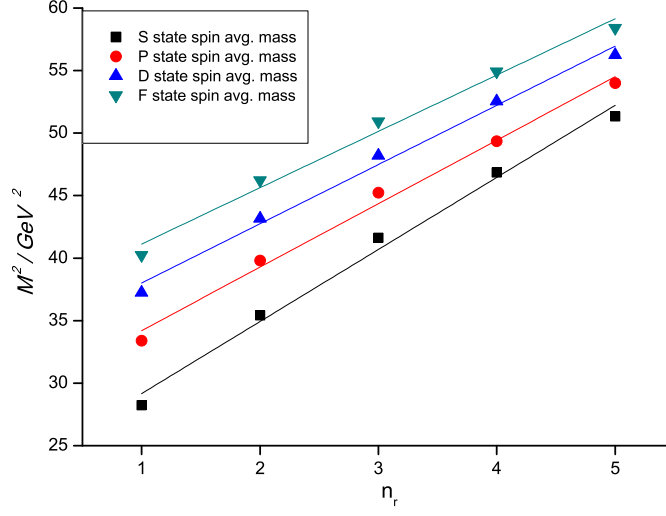


Fig. 4. $n_r \rightarrow M^2$ Regge trajectory for B -meson, spin-average masses

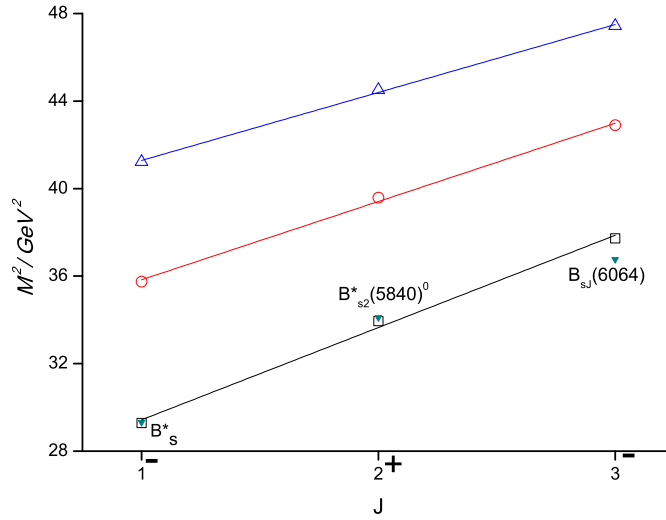


Fig. 5. $J \rightarrow M^2$ Regge trajectory for B_s -meson, natural parity states, hollow shapes indicates present results and solid shapes indicates experimental results

and

$$x_b = \left(3 - 2 \frac{m_{B^-}}{m_b} \right)^2 \quad (22)$$

The rare di-leptonic decay width for B_s^0 and B^0 mesons is given by [69, 70]. Our calculated rare dileptonic decay width can be found in Tables 17 & 18.

$$\Gamma(B_q^0 \rightarrow l^+ l^-) = \frac{G_F^2}{\pi} \left(\frac{\alpha}{4\pi \sin^2 \Theta_W} \right)^2 f_{B_q}^2 m_l^2 m_{B_q} \times \sqrt{1 - 4 \frac{m_l^2}{m_{B_q}^2}} |V_{tq}^* V_{tb}|^2 |C_{10}|^2 \quad (23)$$

The branching ratio for $B_q^0 \rightarrow l^+ l^-$ is

$$BR \rightarrow \Gamma_{(B_q^0 \rightarrow l^+ l^-)} \times \tau_{B_q} \quad (24)$$

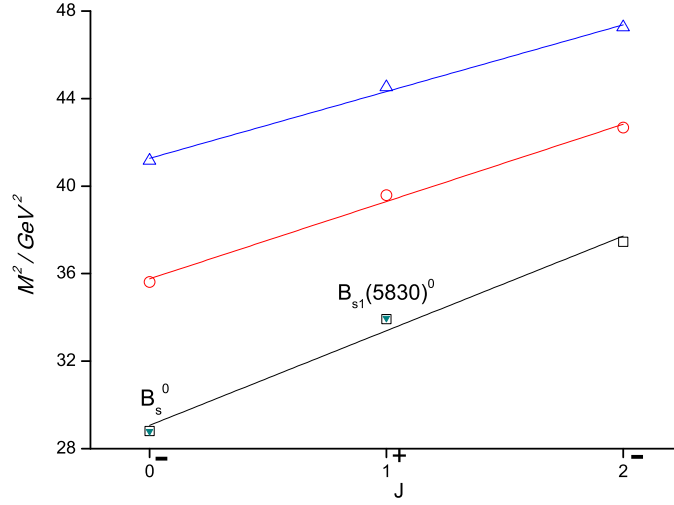


Fig. 6. $J \rightarrow M^2$ Regge trajectory for B_s -meson, natural parity states, hollow shapes indicates present results and solid shapes indicates experimental results

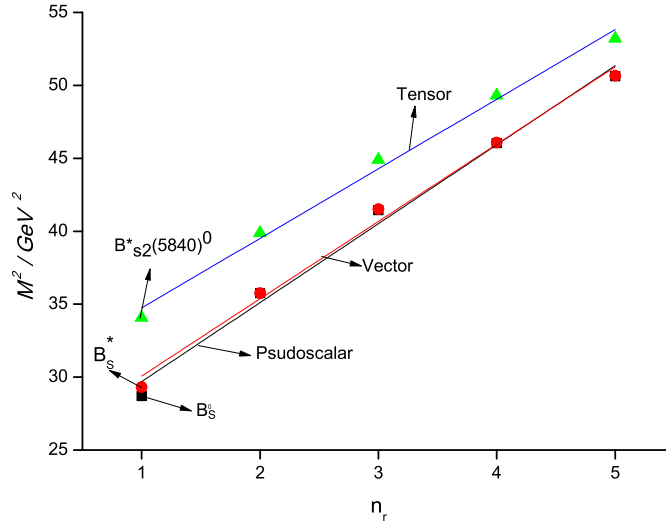


Fig. 7. $n_r \rightarrow M^2$ Regge trajectory for B_s -meson, , pseudoscalar, vector and tensor states

C_{10} is the Wilson coefficient given by [71,72], f_{B_q} is the corresponding decay constant, and G_F is the Fermi coupling constant. We have considered $\tau_B = 1.638$ ps and $\tau_{B_s} = 1.510$ ps.

$$C_{10} = \eta_Y \frac{x_t}{8} \left[\frac{x_t + 2}{x_t - 1} + \frac{3x_t - 6}{(x_t - 1)^2} \ln x_t \right] \quad (25)$$

$\Theta_W (\approx 28^\circ)$ is the weak mixing angle (Weinberg angle)[73], $\eta_Y (= 1.026)$ is the next-to-leading-order correction[71], and $x_t = (m_t/m_w)^2$.

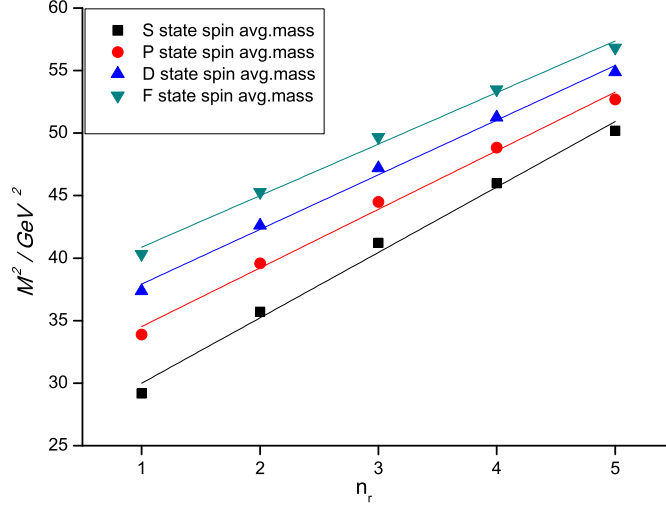


Fig. 8. $J \rightarrow M^2$ Regge trajectory for B_s -meson, , spin-average masses

Table 11. Fitted parameters of the (J, M^2) parent and daughter Regge trajectories for B and B_s - mesons with natural and un-natural parity.

Parity	Meson	Trajectory	$\alpha(\text{GeV}^{-2})$	α_0
Natural	B	Parent	0.217 ± 0.002	-5.167 ± 0.067
		1^{st} daughter	0.255 ± 0.003	-8.048 ± 0.125
		2^{nd} daughter	0.296 ± 0.001	-11.260 ± 0.052
Un-natural	B^*	Parent	0.217 ± 0.021	-6.14 ± 0.707
		1^{st} daughter	0.263 ± 0.018	-9.315 ± 0.725
		2^{nd} daughter	0.306 ± 0.017	-12.706 ± 0.784
Natural	B_s	Parent	0.236 ± 0.014	-5.951 ± 0.477
		1^{st} daughter	0.279 ± 0.011	-8.998 ± 0.453
		2^{nd} daughter	0.321 ± 0.001	-12.279 ± 0.466
Un-natural	B_s^*	Parent	0.228 ± 0.024	-6.638 ± 0.811
		1^{st} daughter	0.281 ± 0.020	-10.069 ± 0.799
		2^{nd} daughter	0.326 ± 0.019	-13.48 ± 0.859

Table 12. Fitted parameters of the (n_r, M^2) Regge trajectories for B and B_s -mesons

Mesons	$\beta(\text{GeV}^{-2})$	β_0
B^0	0.169 ± 0.009	-3.869 ± 0.413
B^*	0.173 ± 0.009	-4.050 ± 0.388
$B_2^*(5747)^0$	0.193 ± 0.009	-5.58 ± 0.448
B_s^0	0.183 ± 0.010	-4.416 ± 0.423
B_s^*	0.187 ± 0.008	-4.623 ± 0.360
$B_{s2}^*(5840)^0$	0.208 ± 0.009	-6.627 ± 0.424

Table 13. Fitted parameters of the (n_r, M^2) S, P, D and F state spin-average mass Regge trajectories for B and B_s - mesons.

Meson	Trajectory	$\beta(GeV^{-2})$	β_0
B	S State	0.155 ± 0.015	-4.187 ± 0.642
	P State	0.195 ± 0.01	-6.631 ± 0.446
	D State	0.212 ± 0.011	-7.973 ± 0.526
	F State	0.226 ± 0.012	-9.273 ± 0.638
B_s	S State	0.189 ± 0.009	-5.673 ± 0.395
	P State	0.212 ± 0.009	-7.310 ± 0.418
	D State	0.227 ± 0.009	-8.623 ± 0.458
	F State	0.241 ± 0.010	-9.841 ± 0.538

Table 14. Decay Constant of pseudoscalar and vector states of B and B_s meson (in GeV).

Model	1S	2S	3S	4S	5S	
B	f_{Pcor}	0.149	0.071	0.045	0.033	0.025
	f_p	0.154	0.073	0.046	0.034	0.026
	[56]	0.188 ± 25				
	[16]	0.146	0.105	0.086	0.074	0.066
	[60]	0.155 ± 0.015				
B^*	f_{Vcor}	0.150	0.071	0.045	0.033	0.025
	f_V	0.155	0.071	0.046	0.034	0.026
	[16]	0.146	0.105	0.086	0.074	0.066
	[61]	0.196				
	[62,63]	0.175				
B_s	f_{Pcor}	0.191	0.089	0.0570	0.0413	0.0327
	f_p	0.210	0.098	0.0628	0.0454	0.0359
	[64]	0.237 ± 0.0147				
	[16]	0.187	0.134	0.110	0.095	0.085
	[44]	0.232	0.107	0.077	0.062	
B_s^*	[60]	0.210 ± 0.020				
	f_{Vcor}	0.192	0.089	0.0572	0.0413	0.0327
	f_V	0.211	0.098	0.0629	0.0454	0.0359
	[16]	0.187	0.134	0.110	0.095	0.085
	[65,66]	0.213 ± 0.018				
[62,63]	0.213					

Table 15. Leptonic Branching fraction of the B meson.

State	$B^+ \rightarrow \tau^+ \nu_\tau$ Br_τ	$B^+ \rightarrow \mu^+ \nu_\mu$ Br_μ	$B^+ \rightarrow e^+ \nu_e$ Br_e
Present	0.0285×10^{-4}	0.128×10^{-7}	0.3×10^{-12}
[56]	$(1.09 \pm 0.24) \times 10^{-4}$	$< 1.0 \times 10^{-6}$ (CL= 90%)	$< 9.8 \times 10^{-7}$ (CL=90%)
[16]	0.822×10^{-4}	0.37×10^{-7}	8.64×10^{-12}
[57]	1.354×10^{-4}		
[74]	1.1×10^{-4}	4.7×10^{-7}	1.11×10^{-11}
[44]	1.13×10^{-11}	4.82×10^{-7}	1.07×10^{-7}

6 Mixing Parameters

Many experiments[82,83] have reported neutral open beauty meson oscillations. Using the spectroscopic parameters from the present study we calculate the mass oscillation of the neutral open beauty meson and integrated oscillation rate. We use the notation available in[84] and also consider CPT conservation. Time evolution of the neutral B and

Table 16. Branching ratio with corresponding radiative leptonic decay width

Meson	Γ/GeV	BR					
		Present	[16]	[75]	[76]	[77]	
B	f_p	1.23×10^{-19}	0.30×10^{-6}	0.38×10^{-6}	0.23×10^{-6}	1.66×10^{-6}	5.21×10^{-6}
	f_{pcor}	0.19×10^{-19}	0.47×10^{-7}	0.34×10^{-6}			
B_s	f_p	2.49×10^{-19}	6.21×10^{-7}				
	f_{pcor}	5.24×10^{-20}	1.30×10^{-7}				

Table 17. Branching ratio with corresponding rare leptonic decay width of the B^0 meson.

Process	$\Gamma(B_q^0 \rightarrow l^+ l^-)(keV)$		BR	
	Present	Others	Present	Others
$B^0 \rightarrow \mu^+ \mu^-$	2.49×10^{-17}	4.34×10^{-17} [16] 4.41×10^{-17} [57]	5.75×10^{-11}	$(3.9_{-1.4}^{+1.6}) \times 10^{-10}$ [64] 1.018×10^{-10} [57] 1.00×10^{-10} [16] $< 1.1 \times 10^{-9}$ [78]
$B^0 \rightarrow \tau^+ \tau^-$	5.22×10^{-15}	9.10×10^{-10} [16] 9.23×10^{-10} [57]	1.20×10^{-8}	$< 4.1 \times 10^{-3}$ [64] 2.133×10^{-8} [57] 2.10×10^{-8} [16] $(2.22 \pm 0.19) \times 10^{-8}$ [79] 2.52×10^{-8} [80]
$B^0 \rightarrow e^+ e^-$	5.84×10^{-22}	1.02×10^{-21} [16] 1.03×10^{-21} [57]	1.34×10^{-15}	$< 8.3 \times 10^{-8}$ [64] 2.376×10^{-15} [57] 2.35×10^{-15} [16] $(2.48 \pm 0.21) \times 10^{-15}$ [79] 2.82×10^{-15} [80]

Table 18. Branching ratio with corresponding rare leptonic decay width of the B_s^0 meson.

Process	$\Gamma(B_q^0 \rightarrow l^+ l^-)(keV)$		BR	
	Present	Others	Present	Others
$B_s^0 \rightarrow \mu^+ \mu^-$	4.70×10^{-17}	1.10×10^{-15} [16] 1.58×10^{-15} [57]	1.08×10^{-10}	$(2.9_{-0.6}^{+0.7}) \times 10^{-9}$ [64] 3.602×10^{-9} [57] 2.53×10^{-9} [16] $(3.0_{-0.9}^{+1.0}) \times 10^{-9}$ [78] $(2.9_{-1.0}^{+1.1}) \times 10^{-9}$ [81]
$B_s^0 \rightarrow \tau^+ \tau^-$	9.97×10^{-15}	2.34×10^{-13} [16] 3.36×10^{-13} [57]	2.30×10^{-8}	7.647×10^{-7} [80] 7.647×10^{-7} [57] 5.36×10^{-7} [16] $(7.73 \pm 0.023) \times 10^{-7}$ [79]
$B_s^0 \rightarrow e^+ e^-$	1.10×10^{-21}	2.58×10^{-21} [16] 3.70×10^{-20} [57]	2.54×10^{-15}	$< 2.8 \times 10^{-7}$ [64] 8.408×10^{-14} [57] 5.92×10^{-14} [16] $(8.54 \pm 0.55) \times 10^{-14}$ [79] 7.97×10^{-14} [80]

B_s meson doublet is described by the Schrodinger equation[85].

$$i \frac{d}{dt} \begin{pmatrix} D_q \\ \bar{D}_q \end{pmatrix} = \left[\begin{pmatrix} M_{11}^q & M_{12}^{q*} \\ M_{12}^q & M_{11}^q \end{pmatrix} - \frac{i}{2} \begin{pmatrix} \Gamma_{11}^q & \Gamma_{12}^{q*} \\ \Gamma_{12}^q & \Gamma_{11}^q \end{pmatrix} \right] \begin{pmatrix} D_q \\ \bar{D}_q \end{pmatrix} \quad (26)$$

The off-diagonal elements of the mass and decay matrices are[86]

$$M_{12} = - \frac{G_F^2 m_W^2 \eta_D m_{D_q} B_{D_q} f_{D_q}^2 S_0 (m_s^2 / m_W^2) (V_{us}^* V_{cs})^2}{12\pi^2} \quad (27)$$

Table 19. Mixing of B and B_s mesons variables.

States	$\Delta m_q \times 10^{-12}$	x_q	y_q	χ_q	R_M
Present (B)	0.25374	0.415627	1.281×10^{-3}	0.073	0.086
[56]	0.5064 ± 0.0019	0.770 ± 0.004		1.860 ± 0.0011	
[16]	0.5397	0.8841	2.63×10^{-3}	0.2199	0.3909
[57]	0.506	0.769			
[44]	0.498	0.759	2.6×10^{-3}	0.2242	
Present (B_s)	25.37	12.68	3.81×10^{-3}	0.00079	0.0080
[56]	17.757 ± 0.021	26.79 ± 0.08		0.499307 ± 0.000004	
[16]	14.13	21.36	5.40×10^{-2}	0.4989	228.23
[57]		17.644	26.41	8.9×10^{-2}	0.4993
[90]	17.30 ± 2.6				
[91]	15.8				

$$\Gamma_{12} = \frac{G_F^2 m_c^2 \eta_D' m_{D_q} B_{D_q} f_{D_q}^2}{8\pi} [(V_{us}^* V_{cs})^2] \quad (28)$$

Here, m_W is the W boson mass, m_b is the mass of b -quark, G_f is Fermi constant, and m_{B_q} , f_{B_q} and B_{B_q} are the B_q mass, the weak decay constant and the bag parameter, respectively. V_{ij} are the CKM matrix elements and $S_0(x_t)$ [87] can be approximated as $0.784x_t^{0.76}$ [88]. η_D and η_D' resemble gluonic corrections. τ_B (hadronic lifetime) is related to Γ_{11}^q ($\tau_{B_q} = 1/\Gamma_{11}^q$), and Δm_q and $\Delta \Gamma_q$ are related to M_{12}^q and Γ_{12}^q [89].

$$\Delta m_q = 2 |M_{12}^q| \quad (29)$$

and

$$\Delta \Gamma_q = 2 |\Gamma_{12}^q| \quad (30)$$

χ_q (integrated oscillation rate) is the probability of observing a \bar{B}_q meson in a jet initiated by \bar{b} quark, Δm_{B_q} is a measure of frequency of the change from a B_q into a \bar{B}_q or vice versa.

The ratio;

$$r_o = \frac{B_q \leftrightarrow \bar{B}_q}{B_q \leftrightarrow B_q} = \frac{\int_0^\infty |g_-(t)|^2 dt}{\int_0^\infty |g_+(t)|^2 dt} = \frac{x^2}{2+x^2}, \quad (31)$$

$$|g_\pm(t)|^2 = \frac{1}{2} e^{-\frac{\Gamma_D t}{2}} [1 \pm \cos(t\Delta m)]. \quad (32)$$

$$\text{where } x_q = x = \frac{\Delta m}{\Gamma} = \Delta m \tau_D, \quad y_q = \frac{\Delta \Gamma}{2\Gamma} = \frac{\Delta \Gamma}{2} \tau_D,$$

$$\chi_q = \frac{x_q^2 + y_q^2}{2(x_q^2 + 1)}, \quad (33)$$

In the absence of CP violation, we have the time-integrated mixing rate for semi-leptonic decays as

$$R_M \simeq \frac{1}{2}(x_q^2 + y_q^2). \quad (34)$$

For present computation of the mixing parameters, we employ our calculated value for Δm and experimental average lifetime from PDG. The computed values of mixing parameters can be found in Table 19.

7 Electromagnetic transition widths

The electromagnetic transition width help to understand the non-perturbative characteristic of QCD. $\Delta L = \pm 1$ and $\Delta S = 0$ and, $\Delta L = 0$ and $\Delta S = \pm 1$ are the selection rules for calculating the electric and magnetic transition widths. We use the variational radial wave-functions for initial and final states to calculate electromagnetic transition widths. In non-relativistic limit the, widths can be calculated as per[92,93,94,95] and the calculated results can be found in Tables 20,21 and 22.

$$\Gamma(n^{2S+1}L_iJ_i \rightarrow n^{2S+1}L_fJ_f + \gamma) = \frac{4\alpha_e \langle e_Q \rangle^2 \omega^3}{3} (2J_f + 1) S_{if}^{E1} |M_{if}^{E1}|^2 \quad (35)$$

$$\Gamma(n^3S_1 \rightarrow n^1S_0 + \gamma) = \frac{\alpha_e \mu^2 \omega^3}{3} (2J_f + 1) S_{if}^{M1} |M_{if}^{M1}|^2 \quad (36)$$

Here, $\langle e_Q \rangle$, μ and ω are mean charge content, magnetic dipole moment and photon energy of the system respectively, and are written as,

$$\langle e_Q \rangle = \left| \frac{m_{\bar{q}} e_Q - e_{\bar{q}} m_Q}{m_Q + m_{\bar{q}}} \right| \quad (37)$$

$$\mu = \frac{m_{\bar{q}} e_Q - e_{\bar{q}} m_Q}{m_Q m_{\bar{q}}} \quad (38)$$

$$\omega = \frac{M_i^2 - M_f^2}{2M_i} \quad (39)$$

$$S_{if}^{E1} = \max(L_i, L_f) \left\{ \begin{matrix} J_i & 1 & J_f \\ L_f & S & L_i \end{matrix} \right\}^2 \quad (40)$$

and

$$S_{if}^{M1} = 6(2S_i + 1)(2S_f + 1) \left\{ \begin{matrix} J_i & 1 & J_f \\ S_f & \ell & S_i \end{matrix} \right\}^2 \left\{ \begin{matrix} 1 & \frac{1}{2} & \frac{1}{2} \\ \frac{1}{2} & S_f & S_i \end{matrix} \right\}^2. \quad (41)$$

The matrix element $|M_{if}|$ for $E1$ and $M1$ transitions can be written as

$$|M_{if}^{E1}| = \frac{3}{\omega} \left\langle f \left| \frac{\omega r}{2} j_0 \left(\frac{\omega r}{2} \right) - j_1 \left(\frac{\omega r}{2} \right) \right| i \right\rangle \quad (42)$$

and

$$|M_{if}^{M1}| = \left\langle f \left| j_0 \left(\frac{\omega r}{2} \right) \right| i \right\rangle \quad (43)$$

8 Results, Discussion and Conclusion

In present article we have calculated the B and B_s meson spectrum in semi-relativistic approach. We have added relativistic correction to the kinetic energy and potential energy terms in the potential, for the present work we have used the screening potential. Numerical values of various orders of relativistic corrections for B and B_s meson can be found in Table 3. The Gaussian like wave-function in position and momentum space has been used, and the potential has been solved using the variational approach. The spin average masses and the masses for s, p, d & f states of B and B_s meson can be found in Tables 6,7,8,9,10, respectively. On analyzing the masses, it is evident that for states $n \geq 3$ the spin-average masses for the present study are suppressed in comparison to [16](semi-relativistic approach, but using Cornell potential). The masses calculated in the present article are consistent with the masses calculated by Relativistic quark model[17], Godfrey Isgur model[21], Godfrey Isgur model along with screened potential model[99], and R.Q.M based on a heavy-quark expansion of the instantaneous Bethe-Salpeter equation[27].

It is well proven fact that $B_J^*(5732)$, first observed at OPAL detector, later separated into two states $B_1(5721)^0$ and $B_2^*(5747)^0$. For B meson we juxtapose the calculated masses from present approach with experimentally determined masses and masses from other theoretical approaches, as can be seen in Tables 7 & 8. We observe that the two states B^0 and B^* are reproduced well with only a difference of 3 and 0 Mev, respectively in comparison with PDG masses[56].

Table 20. E1 transition of B meson.

State		Recent study				Other study (Γ in keV)		
Initial	Final	$E_\gamma(MeV)$	$\Gamma(keV)$	[16]	[22]	[21]	[44]	
$B(1^3P_2)$	$B(1^3S_1)$	437	315.054	215.39	177.7	444	131.36	
$B(1^3P_1)$	$B(1^3S_1)$	429	316.32	227.09	108.5	300	122.87	
$B(1^1P_1)$	$B(1^1S_0)$	460	390.51	74.66	60.4	132	179.35	
$B(1^1P_1)$	$B(1^3S_1)$	426	310	51.90	53.1	97.5	8.98	
$B(1^1P_1)$	$B(1^1S_0)$	458	383	252.16	130.2	373	6.09	
$B(1^3P_0)$	$B(1^3S_1)$	423	302	201.34	116.9	325	100.54	
$B(2^3S_1)$	$B(1^3P_2)$	201	37.89	34.75	51.6	30.8	10.33	
$B(2^3S_1)$	$B(1^3P_1)$	177	15.49	16.77	25.9	13.7	2.07	
$B(2^3S_1)$	$B(1^1P_1)$	180	16.26	5.82	11.67	5.32	13.79	
$B(2^3S_1)$	$B(1^3P_0)$	184	5.77	7.94	21.4	8.25	0.94	
$B(2^1S_0)$	$B(1^3P_1)$	168	39.93	9.43	25.2	9.01		
$B(2^1S_0)$	$B(1^1P_1)$	171	42.03	49.39	49.6	31.1		
$B(1^3D_3)$	$B(1^3P_2)$	369	641.88	411.7	127	464		
$B(1^1D_2)$	$B(1^3P_2)$	333	118	26.74	57.2	80.5		
$B(1^1D_2)$	$B(1^3P_2)$	296	83.03	59.25	14.5	42.2		
$B(1^3D_1)$	$B(1^3P_2)$	293	8.96	5.94	9.3	13		
$B(1^3D_1)$	$B(1^3P_1)$	269	104.2	73.97	106.2	144		
$B(1^3D_1)$	$B(1^3P_1)$	272	107.6	296.6	49	52.2		
$B(1^3D_1)$	$B(1^3P_0)$	276	149.6	131.38	283.5	297		
$B(1^3D_2)$	$B(1^3P_1)$	309	379	153.8	356.3	433		
$B(1^3D_2)$	$B(1^1P_1)$	312	389	17.6	8.6	29		
$B(1^1D_2)$	$B(1^1P_1)$	272	258	10.4	0.1	2.67		
$B(1^1D_2)$	$B(1^1P_1)$	275	266.6	133.2	143.1	397		
$B(2^3P_2)$	$B(2^3S_1)$	318		319.93		258		
$B(2^3P_1)$	$B(2^3S_1)$	328		340.32		243		
$B(2^3P_1)$	$B(2^1S_0)$	337		30.47		111		
$B(2^1P_1)$	$B(2^3S_1)$	327		83.99		70.5		
$B(2^1P_1)$	$B(2^1S_0)$	335		35.3		208		
$B(2^3P_0)$	$B(2^3S_1)$	325		31.14		66.7		
$B(2^3P_2)$	$B(1^3D_3)$	149	0.6	32.26		16.5		
$B(2^3P_2)$	$B(1^3D_2)$	186	5.21	7.22				
$B(2^3P_2)$	$B(1^1D_2)$	223	9.07	3.05		14.8		
$B(2^3P_2)$	$B(1^3D_1)$	226	2.03	0.88				
$B(2^3P_1)$	$B(1^3D_1)$	237	11.67	6.73		3.68		
$B(2^1P_1)$	$B(1^3D_1)$	235	11.39	20.31				
$B(2^3P_0)$	$B(1^3D_1)$	233	14.82	86.17		16.1		

As per theoretical studies by [18,34,33,16] $B_1(5721)^0$ has been regarded as $B(1^1P_1)$ or $B(1^3P_1)$ state or as an admixture of these two states. But, depending upon our calculated masses and constructed (J, M^2) Regge trajectory in Fig.2 we associate it as 1^1P_1 state, because the calculated mass from the present study show linearity and parallelism and fit well on the parent (J, M^2) trajectory. For $B_2^*(5747)^0$ state, the difference between mass calculated by us and that from PDG[56] is only 0.7% and the constructed (J, M^2) Regge trajectory in Fig.1 helps in associating $B_2^*(5747)^0$ as 1^3P_2 state. It is well understood that $B_J(5960)$ and $B_J(5970)$ are same states, and their masses are nearby the estimated masses of 2^1S_0 and 2^3S_1 states. Because, $B_J(5970)$ decays to $B\pi$, we eliminate its association to 2^1S_0 state. Our calculated mass for $B_J(5970)$ differs from PDG value by 2 Mev only. Thus, helping us relate $B_J(5970)$ as 2^3S_1 state. Also, our present study help us link $B_J(5840)^0$ with 2^1S_0 state. The (n_r, M^2) Regge trajectory in Fig.3 show

Table 21. E1 transition of B_s meson.

State		Recent study				Other study (Γ in keV)		
Initial	Final	E_γ (MeV)	Γ (keV)	[16]	[22]	[21]	[44]	
$B_s(1^3P_2)$	$B_s(1^3S_1)$	407	81.73	150.59	159	106.0	131.36	
$B_s(1^3P_1)$	$B_s(1^3S_1)$	397	80.62	151.14	98.8	57.3	122.87	
$B_s(1^3P_1)$	$B_s(1^1S_0)$	439	108.71	35.59	56.6	47.8	179.35	
$B_s(1^1P_1)$	$B_s(1^3S_1)$	396	80.05	24.64	39.5	36.9	8.98	
$B_s(1^1P_1)$	$B_s(1^1S_0)$	438	108.03	184.92	97.7	70.6	06.09	
$B_s(1^3P_0)$	$B_s(1^3S_1)$	375	68.25	123.75	84.7	76.0	100.54	
$B_s(2^3S_1)$	$B_s(1^3P_2)$	151	5.80	18.81	25.6	8.08	10.33	
$B_s(2^3S_1)$	$B_s(1^3P_1)$	152	3.61	1.069	1.6	3.2	2.07	
$B_s(2^3S_1)$	$B_s(1^1P_1)$	153	3.68	2.34	9.4	2.28	13.79	
$B_s(2^3S_1)$	$B_s(1^3P_0)$	175	1.81	5.64	17.2	2.52	0.94	
$B_s(2^1S_0)$	$B_s(1^1P_1)$	142	8.72	3.58	12.3	4.66		
$B_s(2^1S_0)$	$B_s(1^1P_1)$	143	8.90	26.37	41.7	6.73		
$B_s(1^3D_3)$	$B_s(1^3P_2)$	307	128	249.92	113.2	109.6		
$B_s(1^3D_2)$	$B_s(1^3P_2)$	286	25.94	16.64	31.5	18.8		
$B_s(1^1D_2)$	$B_s(1^3P_2)$	261	19.56	38.93	10.5	10.2		
$B_s(1^3D_1)$	$B_s(1^3P_2)$	261	2.17	4.14	5.1	3.07		
$B_s(1^3D_1)$	$B_s(1^3P_1)$	263	33.32	57.35	56.8	28.5		
$B_s(1^3D_1)$	$B_s(1^1P_1)$	264	33.69	21.46	35.3	19.6		
$B_s(1^3D_1)$	$B_s(1^3P_0)$	285	56.50	109.42	204.4	74.7		
$B_s(1^3D_2)$	$B_s(1^3P_1)$	288	105.8	151.20	195.4	112.0		
$B_s(1^3D_2)$	$B_s(1^1P_1)$	289	106.9	17.01	5.9	1.07		
$B_s(1^1D_2)$	$B_s(1^3P_1)$	263	79.98	1.18	0.04	0.368		
$B_s(1^1D_2)$	$B_s(1^1P_1)$	264	80.85	131.42	138.8	95.9		
$B_s(2^3P_2)$	$B_s(2^3S_1)$	305	86.74	211.55		65.4		
$B_s(2^3P_1)$	$B_s(2^3S_1)$	305	86.74	212.6		52.3		
$B_s(2^3P_1)$	$B_s(2^1S_0)$	315	95.95	12.51		25.2		
$B_s(2^1P_1)$	$B_s(2^3S_1)$	305	86.74	42.78		18.6		
$B_s(2^1P_1)$	$B_s(2^1S_0)$	315	95.95	237.2		50.7		
$B_s(2^3P_0)$	$B_s(2^3S_1)$	291	111	186.64		66.8		
$B_s(2^3P_2)$	$B_s(1^3D_3)$	195	11.0	21.90		5.61		
$B_s(2^3P_2)$	$B_s(1^1D_2)$	169	1.277	4.72				
$B_s(2^3P_2)$	$B_s(1^1D_2)$	195	1.96	1.49				
$B_s(2^3P_2)$	$B_s(1^3D_1)$	148	0.056	0.51				
$B_s(2^3P_1)$	$B_s(1^3D_1)$	195	3.27	2.90		0.944		
$B_s(2^1P_1)$	$B_s(1^3D_1)$	195	3.27	11.51				
$B_s(2^3P_0)$	$B_s(1^3D_1)$	182	10.56	42.98		3.87		

linearity and parallelism with both $B_J(5970)$ and $B_J(5840)^0$ lying on pseudoscalar and vector trajectories, resulting in validating our association of $B_J(5970)$ and $B_J(5840)^0$ as 2^3S_1 and 2^1S_0 states.

In the B_s meson family two $1S$ states B_S and B_S^* are reproduced well. the difference between our calculated masses and that from PDG for these two states differ only by 7 and 0 Mev respectively. $B_{sJ}^*(5850)$ state was first observed at OPAL detector, was later severed into two different states $B_{s1}(5830)^0$ and $B_{s2}^*(5840)^0$. Based on our study of mass spectra and constructed Regge trajectories in Fig.5 and 6 we associate $B_{s1}(5830)^0$ as 1^1P_1 state and $B_{s2}^*(5840)^0$ as 1^3P_2 state. Calculated masses from current study fall within the error margin of the masses determined by Expt.(PDG)[56], and also match well with other theoretical studies. Two new states $B_{sJ}(6064)$ and $B_{sJ}(6114)$ were recently observed at LHCb[100] in the B^+K^- mass spectrum at a mass approximately 300 Mev above B^+K^- threshold. As per mass

Table 22. M1 transition of B and B_s mesons.

State Initial→ Final	Recent study		Other study (Γ in keV)							
	$E_\gamma(MeV)$	$\Gamma(keV)$	[56]	[16]	[22]	[21]	[44]	[96]	[97]	[98]
$B(1^3S_1) \rightarrow B(1^1S_0)$	41	0.135	0.13±0.01	0.069	0.1	1.23	1.258	0.19	0.1472	0.13±0.01
$B(2^3S_1) \rightarrow B(2^1S_0)$	8.99	0.013		0.014	0.05		0.018		0.1458	
$B(3^3S_1) \rightarrow B(3^1S_0)$	3.99	0.11		0.005			0.003			
$B(2^3S_1) \rightarrow B(1^1S_0)$	624	65.078		53.79	8.0	67.4				
$B(2^1S_0) \rightarrow B(1^3S_1)$	616	187.58		124.1	0.9	108				
$B(1^1P_1) \rightarrow B(1^3P_0)$	3.99	0.0001		0.00003	0.03					
$B(1^1P_1) \rightarrow B(1^3P_0)$	6.99	0.000633		0.017	0.01					
$B(1^3P_2) \rightarrow B(1P_1)$	2			0.002	0.0014					
$B(1^1P_1) \rightarrow B(1^3P_2)$	2			0.015	0.017					
$B(1^3D_3) \rightarrow B(1^1D_2)$	2.99	0.000249		1.29	0.7					
$B(1^3D_3) \rightarrow B(1^3D_1)$	38.87			1.479						
$B(1^3D_2) \rightarrow B(1^3D_1)$	41.8	0.402		0.542	0.0023					
$B(1^3D_2) \rightarrow B(1^1D_2)$	38.8	0.538		0.314	1.9					
$B_s(1^3S_1) \rightarrow B_s(1^1S_0)$	55	0.102	0.064±0.016	0.095	0.1	0.313	0.286	0.054		
$B_s(2^3S_1) \rightarrow B_s(2^1S_0)$	10	0.00079		0.018	0.02		0.008		0.0531	
$B_s(3^3S_1) \rightarrow B_s(3^1S_0)$	4.99	0.0000744		0.007			0.001			
$B_s(2^3S_1) \rightarrow B_s(1^1S_0)$	580	16.92		35.06	4	14.2				
$B_s(2^1S_0) \rightarrow B_s(1^3S_1)$	530	38.20		85.03	0.1	3.23				
$B_s(1^1P_1) \rightarrow B_s(1^3P_0)$	2.19	0.063		0.013	0.02					
$B_s(1^1P_1) \rightarrow B_s(1^3P_0)$	2.29	0.0072		0.029	0.05					
$B_s(1^3P_2) \rightarrow B_s(1^1P_1)$	2.99	0.00004		0.005	0.04					
$B_s(1^1P_1) \rightarrow B_s(1^3P_2)$	1.99	0.0000121		0.00011	0.000052					
$B_s(1^3D_3) \rightarrow B_s(1^1D_2)$	0.9			0.445	0.1					
$B_s(1^3D_3) \rightarrow B_s(1^3D_1)$	0.4	0.206		0.462						
$B_s(1^1D_2) \rightarrow B_s(1^3D_1)$	26.94	0.0348		0.168	0.0013					
$B_s(1^3D_2) \rightarrow B_s(1D_2)$	26.94	0.0581		0.125	0.4					

predictions from various quark models these two new states can be good candidates for $1D$ wave states. The calculated mass for 1^1D_2 state for B_s meson from the current study varies only by 0.67% with respect to the experiment mass from LHCb for $B_{S,J}(6064)$ state. The calculated mass fits very well on the parent (J, M^2) Regge trajectory and follows linearity and parallelism. Hence, we associate $B_{S,J}(6064)$ with 1^1D_2 B_s meson state.

According to our analysis, we interpret $B_{S,J}(6114)$ as an admixture of 2^3S_1 (5995 Mev) and 1^3D_1 (6112 Mev) considering mixing angle $\theta = 85^\circ$ we calculate mass of $B_{S,J}(6064)$ as 6111.1 Mev which lies in experimentally determined error bar 6114 ± 5 Mev [100]. More experimental and theoretical analysis is required to throw more light on these two newly observed B_s meson states. We also predict s, p, d & f states for both B and B_s mesons and compare with available theoretical data.

The decay constant for s -wave states for both B and B_s meson have been calculated using the Van-Royen-Weisskopf formula, the first order QCD correction factor has also been incorporated. The calculated decay constant can be found in Table 14. The calculated decay constant considering QCD correction are bit suppressed when compared to decay constant values calculated experimentally.

The calculated values of branching fraction of the B meson is tabulated in Table 15, and compared with theoretically and experimentally determined values. For Br_μ and Br_e our predictions are in accordance with experimentally determined branching fraction values, but for Br_τ the calculated value is suppressed.

Theoretically many methods are available to calculate radiative leptonic decay width and branching ratio, like in Ref.[16] considering non-relativistic quark model, ref.[101] considering perturbative QCD approach, factorization approach in [102,103,104]. In all these approaches the value of branching ratio is in the range of 10^{-6} for B meson. In present study the determined value of branching ratio is of the order 10^{-7} for both the B and B_s meson, the calculated values of branching ratio with corresponding radiative leptonic decay width can be found in Table 16.

In the Tables 17 & 18 is tabulated predicted branching ratio with corresponding rare leptonic ($B_q^0 \rightarrow l^+l^-$) decay width for both the B and B_s meson. The predicted branching ratios for $B^0 \rightarrow \mu^+\mu^-$ and $B_s^0 \rightarrow \mu^+\mu^-$ are in good agreement with CMS and LHCb[105,106,107]. The predicted branching ratio for $B^0 \rightarrow \tau^+\tau^-$ and $B_s^0 \rightarrow \tau^+\tau^-$ agree well with experimental and other theoretical values. But, the branching ratio for $B^0 \rightarrow e^+e^-$ and $B_s^0 \rightarrow e^+e^-$ also agree well with theoretical predictions.

We have also calculated various mixing parameters for both B and B_s meson. Our predicted mass difference Δm_{B_d} (0.253 ps^{-1}) and Δm_{B_d} (25.37 ps^{-1}) is not away from the experimentally determined mass differences. The calculated value of the mixing parameter χ_q for B and B_s meson is 0.415 and 12.68 respectively, the experimental value for mixing parameter are 0.770 ± 0.004 and 26.79 ± 0.08 respectively. Other mixing parameters x_q and y_q can also

be found in Table19. The values of the mixing parameters are suppressed because in the present article we have only considered short distance contributions.

Employing calculated masses and normalised reduced wave-functions the electromagnetic transition widths for B and B_s meson have also been calculated and tabulated in Tables20, 21 & 22. The calculated electromagnetic transition width are compared with experimental and other theoretical widths.

Finally, we conclude that the masses of B and B_s mesons determined in present article using a semi-relativistic approach and considering screening potential are in fine tune with experimental masses wherever applicable and are also comparable with masses from other theoretical approaches. The screening potential suppresses the masses for states with $n \geq 3$. The mass spectroscopy and (n_r, M^2) , (J, M^2) Regge trajectories helps us associate $B_1(5721)^0$, $B_2^*(5747)^0$, $B_J(5970)$, and $B_J(5840)^0$ in the B meson family as $1P_1$, 1^3P_2 , 2^3S_1 and 2^1S_0 states. In the B_s meson family we associate $B_{s1}(5830)^0$, $B_{s2}^*(5840)^0$, $B_{sJ}(6064)$ as 1^1P_1 , 1^3P_2 , and 1^1D_2 states, and $B_{sJ}(6114)$ as an admixture of 2^3S_1 and 1^3D_1 states.

References

1. R. Aaij, et al., Eur. Phys. J. C **81**(7), 601 (2021). DOI 10.1140/epjc/s10052-021-09305-3
2. S.e.a. Behrends, Phys. Rev. Lett. **50**, 881 (1983). DOI 10.1103/PhysRevLett.50.881. URL <https://link.aps.org/doi/10.1103/PhysRevLett.50.881>
3. K.e.a. Han, Phys. Rev. Lett. **55**, 36 (1985). DOI 10.1103/PhysRevLett.55.36. URL <https://link.aps.org/doi/10.1103/PhysRevLett.55.36>
4. R. Akers, et al., Z. Phys. C **66**, 19 (1995). DOI 10.1007/BF01496577
5. G. Abbiendi, et al., Eur. Phys. J. C **23**, 437 (2002). DOI 10.1007/s100520200892
6. V.M. Abazov, et al., Phys. Rev. Lett. **99**, 172001 (2007). DOI 10.1103/PhysRevLett.99.172001
7. T.A. Aaltonen, et al., Phys. Rev. D **90**(1), 012013 (2014). DOI 10.1103/PhysRevD.90.012013
8. R. Aaij, et al., JHEP **04**, 024 (2015). DOI 10.1007/JHEP04(2015)024
9. J. Lee-Franzini, U. Heintz, D.M.J. Lovelock, M. Narain, R.D. Schamberger, J. Willins, C. Yanagisawa, P. Franzini, P.M. Tuts, Phys. Rev. Lett. **65**, 2947 (1990). DOI 10.1103/PhysRevLett.65.2947
10. T. Aaltonen, et al., Phys. Rev. Lett. **100**, 082001 (2008). DOI 10.1103/PhysRevLett.100.082001
11. R. Aaij, et al., Phys. Rev. Lett. **110**(15), 151803 (2013). DOI 10.1103/PhysRevLett.110.151803
12. V.M. Abazov, et al., Phys. Rev. Lett. **100**, 082002 (2008). DOI 10.1103/PhysRevLett.100.082002
13. C. Matteuzzi, I. Belyaev, G. Carboni, N. Harnew, C. Teubert, Eur. Phys. J. H **46**(1), 3 (2021). DOI 10.1140/epjh/s13129-021-00002-z
14. T. Aaltonen, et al., Phys. Rev. Lett. **102**, 102003 (2009). DOI 10.1103/PhysRevLett.102.102003
15. H.Y. Cheng, F.S. Yu, Eur. Phys. J. C **77**(10), 668 (2017). DOI 10.1140/epjc/s10052-017-5252-4
16. V. Kher, N. Devlani, A.K. Rai, Chin. Phys. C **41**(9), 093101 (2017). DOI 10.1088/1674-1137/41/9/093101
17. D. Ebert, R.N. Faustov, V.O. Galkin, Eur. Phys. J. C **66**, 197 (2010). DOI 10.1140/epjc/s10052-010-1233-6
18. H.X. Chen, W. Chen, X. Liu, Y.R. Liu, S.L. Zhu, Rept. Prog. Phys. **80**(7), 076201 (2017). DOI 10.1088/1361-6633/aa6420
19. J.K. Chen, Eur. Phys. J. C **78**(8), 648 (2018). DOI 10.1140/epjc/s10052-018-6134-0
20. Y. Sun, Q.T. Song, D.Y. Chen, X. Liu, S.L. Zhu, Phys. Rev. D **89**(5), 054026 (2014). DOI 10.1103/PhysRevD.89.054026
21. S. Godfrey, K. Moats, E.S. Swanson, Phys. Rev. D **94**(5), 054025 (2016). DOI 10.1103/PhysRevD.94.054025
22. Q.F. Lü, T.T. Pan, Y.Y. Wang, E. Wang, D.M. Li, Phys. Rev. D **94**(7), 074012 (2016). DOI 10.1103/PhysRevD.94.074012
23. I. Asghar, B. Masud, E.S. Swanson, F. Akram, M. Atif Sultan, Eur. Phys. J. A **54**(7), 127 (2018). DOI 10.1140/epja/i2018-12558-6
24. G.L. Yu, Z.G. Wang, Z.Y. Li, Eur. Phys. J. C **79**(9), 798 (2019). DOI 10.1140/epjc/s10052-019-7314-2
25. T.M. Aliev, M. Savci, Phys. Rev. D **99**(1), 015020 (2019). DOI 10.1103/PhysRevD.99.015020
26. L.F. Gan, M.Q. Huang, Phys. Rev. D **82**, 054035 (2010). DOI 10.1103/PhysRevD.82.054035
27. J.B. Liu, C.D. Lu, Eur. Phys. J. C **77**(5), 312 (2017). DOI 10.1140/epjc/s10052-017-4867-9
28. M.H. Alhakami, Phys. Rev. D **103**(3), 034009 (2021). DOI 10.1103/PhysRevD.103.034009
29. S. Godfrey, N. Isgur, Phys. Rev. D **32**, 189 (1985). DOI 10.1103/PhysRevD.32.189
30. J. Zeng, J.W. Van Orden, W. Roberts, Phys. Rev. D **52**, 5229 (1995). DOI 10.1103/PhysRevD.52.5229
31. M. Di Pierro, E. Eichten, Phys. Rev. D **64**, 114004 (2001). DOI 10.1103/PhysRevD.64.114004
32. P. Gupta, A. Upadhyay, PoS **Hadron2017**, 025 (2018). DOI 10.22323/1.310.0025
33. Q. li, R.H. Ni, X.H. Zhong, (2021)
34. G.L. Yu, Z.G. Wang, Chin. Phys. C **44**(3), 033103 (2020). DOI 10.1088/1674-1137/44/3/033103
35. L.Y. Xiao, X.H. Zhong, Phys. Rev. D **90**(7), 074029 (2014). DOI 10.1103/PhysRevD.90.074029
36. S. Behrends, K. Chadwick, J. Chauveau, P. Ganci, T. Gentile, J.M. Guida, J.A. Guida, R. Kass, A. Melissinos, S. Olsen, et al., Physical Review Letters **50**(12), 881 (1983)
37. J. Lee-Franzini, U. Heintz, D. Lovelock, M. Narain, R. Schamberger, J. Willins, C. Yanagisawa, P. Franzini, P. Tuts, Physical review letters **65**(24), 2947 (1990)
38. K. Han, C. Klopfenstein, G. Mageras, H. Dietl, G. Eigen, V. Fonseca, P. Franzini, J. Horstkotte, R. Imlay, J. Lee-Franzini, et al., Physical review letters **55**(1), 36 (1985)

39. R. Aaij, B. Adeva, M. Adinolfi, A. Affolder, Z. Ajaltouni, S. Akar, J. Albrecht, F. Alessio, M. Alexander, S. Ali, et al., *Journal of High Energy Physics* **2015**(4), 24 (2015)
40. T. Aaltonen, S. Amerio, D. Amidei, A. Anastassov, A. Annovi, J. Antos, G. Apollinari, J. Appel, T. Arisawa, A. Artikov, et al., *Physical Review D* **90**(1), 012013 (2014)
41. R. Aaij, C.A. Beteta, A. Adametz, B. Adeva, M. Adinolfi, C. Adrover, A. Affolder, Z. Ajaltouni, J. Albrecht, F. Alessio, et al., *Physical review letters* **110**(15), 151803 (2013)
42. R. Barate, D. Buskulic, D. Decamp, P. Ghez, C. Goy, J.P. Lees, A. Lucotte, E. Merle, M.N. Minard, J.Y. Nief, et al., *Physics Letters B* **425**(1-2), 215 (1998)
43. O. collaboration, R. Akers, et al., CERN PPE94-206, and Delphi Collaboration, Observation of Orbitally Excited B Mesons, CERN PPE94-210 (1994)
44. N. Devlani, A.K. Rai, *Phys. Rev. D* **84**, 074030 (2011)
45. Y. Koma, M. Koma, H. Wittig, *Phys. Rev. Lett.* **97**, 122003 (2006)
46. E. Eichten, et al., *Rev. Mod. Phys.* **80**, 1161 (2008)
47. E. Laermann, et al., *Phys. Lett. B* **173**, 437 (1986)
48. K. Born, E. Laermann, N. Pirch, T. Walsh, P. Zerwas, *Phys. Rev. D* **40**, 1653 (1989)
49. R. Chaturvedi, et al., *Journal of Physics G: Nuclear and Particle Physics* **47**(11), 115003 (2020)
50. A.M. Badalian, A.I. Veselov, B.L.G. Bakker, *Phys. Rev. D* **70**, 016007 (2004)
51. Y. Simonov, *Phys. Atom. Nucl.* **58**, 107 (1995)
52. D. Ebert, R.N. Faustov, V.O. Galkin, *Phys. Rev. D* **79**, 114029 (2009)
53. D.S. Hwang, G.H. Kim, *Phys. Rev. D* **55**, 6944 (1997)
54. A.K. Rai, et al., *Phys. Rev. C* **78**, 055202 (2008)
55. E.J. Eichten, C. Quigg, *Phys. Rev. D* **49**, 5845 (1994)
56. M. Tanabashi, et al., *Phys. Rev. D* **98**(3), 030001 (2018)
57. M. Shah, B. Patel, P. Vinodkumar, *Physical Review D* **93**(9), 094028 (2016)
58. R. Van Royen, V. Weisskopf, *Nuovo Cim. A* **50**, 617 (1967). [Erratum: *Nuovo Cim.A* 51, 583 (1967)]
59. E. Braaten, S. Fleming, *Phys. Rev. D* **52**, 181 (1995)
60. S. Capstick, S. Godfrey, *Physical Review D* **41**(9), 2856 (1990)
61. R. Verma, *Journal of Physics G: Nuclear and Particle Physics* **39**(2), 025005 (2012)
62. R. Dowdall, C. Davies, R. Horgan, C. Monahan, J. Shigemitsu, H. Collaboration, et al., *Physical review letters* **110**(22), 222003 (2013)
63. B. Colquhoun, C. Davies, J. Kettle, J. Koponen, A. Lytle, R. Dowdall, G. Lepage, H. Collaboration, et al., *Physical Review D* **91**(11), 114509 (2015)
64. C. Patrignani, K. Agashe, G. Aielli, C. Amsler, M. Antonelli, D. Asner, H. Baer, S. Banerjee, R. Barnett, T. Basaglia, et al., (2016)
65. W. Lucha, D. Melikhov, S. Simula, *Physics Letters B* **735**, 12 (2014)
66. W. Lucha, D. Melikhov, S. Simula, *Physical Review D* **91**(11), 116009 (2015)
67. D. Silverman, H. Yao, *Phys. Rev. D* **38**, 214 (1988)
68. C.D. Lu, G.L. Song, *Phys. Lett. B* **562**, 75 (2003)
69. C. Bobeth, M. Gorbahn, T. Hermann, M. Misiak, E. Stamou, M. Steinhauser, *Phys. Rev. Lett.* **112**, 101801 (2014). DOI 10.1103/PhysRevLett.112.101801
70. C. Bobeth, M. Gorbahn, E. Stamou, *Phys. Rev. D* **89**(3), 034023 (2014). DOI 10.1103/PhysRevD.89.034023
71. M. Shah, B. Patel, P.C. Vinodkumar, *Phys. Rev. D* **93**(9), 094028 (2016). DOI 10.1103/PhysRevD.93.094028
72. G. Buchalla, A.J. Buras, *Nucl. Phys. B* **400**, 225 (1993). DOI 10.1016/0550-3213(93)90405-E
73. H.S. Lee, *J. Univ. Sci. Tech. China* **46**(6), 470 (2016). DOI 10.3969/j.issn.0253-2778.2016.06.004
74. J. Fu, H.B. Li, X. Qin, M.Z. Yang, *Modern Physics Letters A* **27**(38), 1250223 (2012)
75. G.P. Korchemsky, D. Pirjol, T.M. Yan, *Physical Review D* **61**(11), 114510 (2000)
76. J.C. Yang, M.Z. Yang, *Nuclear Physics B* **889**, 778 (2014)
77. J.C. Yang, M.Z. Yang, *Nuclear Physics B* **914**, 301 (2017)
78. S. Chatrchyan, V. Khachatryan, A. Sirunyan, A. Tumasyan, W. Adam, T. Bergauer, M. Dragicovic, J. Erö, C. Fabjan, M. Friedl, et al., *Physical review letters* **111**(10), 101804 (2013)
79. C. Bobeth, M. Gorbahn, T. Hermann, M. Misiak, E. Stamou, M. Steinhauser, *Physical review letters* **112**(10), 101801 (2014)
80. P. Dimopoulos, R. Frezzotti, G. Herdoiza, V. Lubicz, C. Michael, D. Palao, G. Rossi, F. Sanfilippo, A. Shindler, S. Simula, et al., *Journal of High Energy Physics* **2012**(1), 1 (2012)
81. R. Aaij, B. Adeva, M. Adinolfi, C. Adrover, A. Affolder, Z. Ajaltouni, J. Albrecht, F. Alessio, M. Alexander, S. Ali, et al., *Physical review letters* **111**(10), 101805 (2013)
82. A. Abulencia, et al., *Phys. Rev. Lett.* **97**, 062003 (2006). DOI 10.1103/PhysRevLett.97.062003
83. P.T. Komiske, E.M. Metodiev, J. Thaler, *JHEP* **07**, 006 (2020). DOI 10.1007/JHEP07(2020)006
84. P.A. Zyla, et al., *PTEP* **2020**(8), 083C01 (2020). DOI 10.1093/ptep/ptaa104
85. G. Buchalla, et al., *Eur. Phys. J. C* **57**, 309 (2008). DOI 10.1140/epjc/s10052-008-0716-1
86. A. Buras, W. Slominski, H. Steger, *Nucl. Phys. B* **245**, 369 (1984)
87. M. Kobayashi, T. Maskawa, *Prog. Theor. Phys.* **49**, 652 (1973). DOI 10.1143/PTP.49.652
88. K. Cichy, M. Kalinowski, M. Wagner, *Phys. Rev. D* **94**(9), 094503 (2016). DOI 10.1103/PhysRevD.94.094503

89. M. Tanabashi, et al., Phys. Rev. D **98**(3), 030001 (2018). DOI 10.1103/PhysRevD.98.030001
90. A. Lenz, U. Nierste, arXiv preprint arXiv:1102.4274 (2011)
91. J. Lahkar, D. Choudhury, B. Hazarika, arXiv preprint arXiv:1902.02079 (2019)
92. N. Brambilla, et al., Eur. Phys. J. **C71**, 1534 (2011)
93. S.F. Radford, W.W. Repko, Nucl. Phys. **A865**, 69 (2011)
94. E. Eichten, K. Gottfried, T. Kinoshita, J.B. Kogut, K.D. Lane, T.M. Yan, Phys. Rev. Lett. **34**, 369 (1975). [Erratum: Phys. Rev. Lett.36,1276(1976)]
95. E. Eichten, K. Gottfried, T. Kinoshita, K.D. Lane, T.M. Yan, Phys. Rev. **D17**, 3090 (1978). [Erratum: Phys. Rev.D21,313(1980)]
96. D. Ebert, R. Faustov, V. Galkin, Physics Letters B **537**(3-4), 241 (2002)
97. S. Bhatnagar, E. Gebrehana, Physical Review D **102**(9), 094024 (2020)
98. H.M. Choi, Physical Review D **75**(7), 073016 (2007)
99. D. Ebert, R.N. Faustov, V.O. Galkin, The European Physical Journal C **66**(1-2), 197–206 (2010)
100. R. Aaij, et al., Eur. Phys. J. C **81**(7), 601 (2021). DOI 10.1140/epjc/s10052-021-09305-3
101. G.P. Korchemsky, D. Pirjol, T.M. Yan, Phys. Rev. D **61**, 114510 (2000). DOI 10.1103/PhysRevD.61.114510
102. M.Z. Yang, Eur. Phys. J. C **72**, 1880 (2012). DOI 10.1140/epjc/s10052-012-1880-x
103. J.C. Yang, M.Z. Yang, Nucl. Phys. B **889**, 778 (2014). DOI 10.1016/j.nuclphysb.2014.10.027
104. J.C. Yang, M.Z. Yang, Nucl. Phys. B **914**, 301 (2017). DOI 10.1016/j.nuclphysb.2016.11.012
105. S. Chatrchyan, et al., Phys. Rev. Lett. **111**, 101804 (2013). DOI 10.1103/PhysRevLett.111.101804
106. R. Aaij, et al., Phys. Rev. Lett. **111**, 101805 (2013). DOI 10.1103/PhysRevLett.111.101805
107. V. Khachatryan, et al., Nature **522**, 68 (2015). DOI 10.1038/nature14474

